CHEMISTRY OF MATERIALS
Article

Chem. Mater. **2009,** *21,* 3987–3995 3987
DOI:10.1021/cm901349y

Single-Crystalline Co Nanowires: Synthesis, Thermal Stability, and Carbon Coating

Diana Ciuculescu,[†,‡] Frédéric Dumestre,[§] Miguel Comesaña-Hermo,[†,‡] Bruno Chaudret,[†,‡] Marina Spasova,[⊥] Michael Farle,[⊥] and Catherine Amiens*[,†,‡]

[†]*CNRS, Laboratoire de Chimie de Coordination, 205 route de Narbonne, F-31077 Toulouse, France,* [‡]*Université de Toulouse, UPS, INPT; LCC; F-31077 Toulouse, France,* [§]*NANOMEPS, 135 avenue de Rangueil,31400 Toulouse, France, and* [⊥]*Fachbereich Physik and Center for Nanointegration, Universität Duisburg-Essen, Lotharstrasse 1, 47048 Duisburg, Germany*

Received May 15, 2009. Revised Manuscript Received July 15, 2009

Decomposition of the organometallic Co(η^3-C_8H_{13})(η^4-C_8H_{12}) complex in the presence of a 2/1 acid/amine mixture, or of cobalt stearate in the presence of 2 equiv. of amine leads to single-crystalline hcp cobalt nanowires of a few nanometers in diameter and micrometers in length. These nanowires display high coercive fields (1.7 T) as well as the magnetization of bulk cobalt. To develop a method for the carbon coating of these nanowires and thus ensure their long-term air stability, the thermal stability of the nanowires is investigated. After being annealed at temperatures above 350 °C under static argon atmosphere, chains of cobalt nanoparticles embedded in a wirelike carbon matrix are obtained. This phenomenon is a consequence of the Rayleigh instability of the nanowires, which is enhanced during the decomposition of the stabilizing ligands. In high-vacuum conditions, in situ transmission electron microscopy (TEM) and high-resolution TEM studies show that the nanowires evaporate without any appearance of Rayleigh instability, and without any structural change. This suggests the crucial role played by the ligands in the fragmentation process. Annealing below 350 °C prevents the fragmentation process and yields carbon-coated cobalt nanowires.

1. Introduction

The ever increasing demand for flexible permanent magnets prompts the development of magnetic materials of high magnetic power (high magnetization and anisotropy). The synthesis of air-stable, oxide-free anisotropic nano-objects, which would be processable into flexible permanent magnets via dispersion in a suitable polymer matrix is thus of great importance and technological relevance. Magnetic nano-objects of anisotropic shape can be prepared via confinement of the growth process inside anisotropic channels,[1−3] via the use of unidirectional substrates such as carbon nanotubes[4,5] or can also be achieved directly via solution phase synthesis. Previous results in this field cover the synthesis of Fe[6,7] or Ni[8] nanorods, Co or CoNi nanowires,[9,10] and cobalt nanodisks.[11] In our group, the synthesis of single-crystalline cobalt nanorods[12] from the organometallic complex Co(η^3-C_8H_{13})(η^4-C_8H_{12}) in the presence of long-chain carboxylic acid and amine ligands has been reported. The aspect ratio of these nanorods could be tuned by the variation of the synthesis parameters, namely the alkyl chain length of the ligands. These objects are ferromagnetic at room temperature. They display a magnetization close to that of bulk cobalt and coercive fields as high as 0.9 T. Furthermore, when using the same organometallic complex, an increase in the acid/amine ratio led to cobalt nanowires with diameters in the nanometer range and coercive fields around 1.7 T. Both kinds of nano-objects (rods and wires) are soluble in organic solvents and can be aligned in a magnetic field,[13] which opens routes for the formation of oriented arrays of these nano-objects inside polymer matrices. However, their air-reactivity remains a problem for possible applications. In past years, stabilization of magnetic nanoparticles

*To whom correspondence should be addressed. Phone: 33 5 61 33 31 82. Fax: 33 5 61 55 30 03. E-mail: amiens@lcc-toulouse.fr.

(1) Chernysheva, M.; Sapoletova, N.; Eliseev, A.; Lukashin, A.; Tretyakov, Y.; Goernert, P. *Pure Appl. Chem.* **2006**, *78*, 1749.
(2) Zhang, J.; Jones, G.; Shen, T.; Donnelly, S.; Li, G. *J. Appl. Phys.* **2007**, *101*, 054310.
(3) Guan, L.; Shi, Z.; Li, H.; Youb, L.; Gu, Z. *Chem. Commun.* **2004**, *17*, 1988.
(4) Alexandrou, I.; Ang, D. K. H.; Mathur, N. D.; Haq, S.; Amaratunga, G. A. J. *Nano Lett.* **2004**, *4*, 2299.
(5) Correa-Duarte, M. A.; Grzelczak, M.; Salgueirino-Maceira, V.; Giersig, M.; Liz-Marzan, L. M.; Farle, M.; Sierazdki, K.; Diaz, R. *J. Phys. Chem. B* **2005**, *109*, 19060.
(6) Cain, J. L.; Nikles, D. E. *J. Appl. Phys.* **1996**, *79*, 4860.
(7) Park, S.-J.; Kim, S.; Lee, S.; Khim, Z. G.; Char, K.; Hyeon, T. *J. Am. Chem. Soc.* **2000**, *122*, 8581.
(8) Cordente, N.; Amiens, C.; Respaud, M.; Senocq, F.; Casanove, M.-J.; Chaudret, B. *Nano Lett.* **2001**, *1*, 565.
(9) Soumare, Y.; Garcia, C.; Maurer, T.; Chaboussant, G.; Ott, F.; Fiévet, F.; Piquemal, J.-Y.; Viau, G. *Adv. Funct. Mater.* **2009**, *19*, 1.
(10) Ung, D.; Viau, G.; Ricolleau, C.; Warmont, F.; Gredin, P.; Fievet, F. *Adv. Mater.* **2005**, *17*, 338.
(11) Puntes, V. F.; Zanchet, D.; Erdonmez, C. K.; Alivisatos, A. P. *J. Am. Chem. Soc.* **2002**, *124*, 12874.
(12) Dumestre, F.; Chaudret, B.; Amiens, C.; Fromen, M.-C.; Casanove, M.-J.; Renaud, P.; Zurcher, P. *Angew. Chem., Int. Ed.* **2002**, *41*, 4286.
(13) Wetz, F.; Soulantica, K.; Respaud, M.; Falqui, A.; Chaudret, B. *Mater. Sci. Eng., C* **2007**, *27*, 1162.

Published on Web 08/05/2009

against oxidation has been the center of several research efforts because of their future applications in fields such as biomedicine, high density magnetic data storage devices, or catalysis (as magnetic platform for magneto-recovery of the catalysts). Although many encapsulation methods have been reported such as coating with silica or organic polymer shells,[14] it has been already reported that the encapsulation of magnetic materials in metal- or carbon-based shells are the most successful processes for long-term preservation of their magnetic properties.[15−21]

The possibility to burn out the organic ligands stabilizing the Co nanowires reported herein and to form a protective carbon shell motivated us to further study the thermal stability of these nanowires. Because of their reduced size and high surface to volume ratio, metallic nanowires may experience morphological instabilities during heating. Indeed, the so-called Rayleigh-Plateau instability has already been observed for a variety of nanowires, e.g., Cu,[22] Au,[23] and Ag.[24] This instability observed for nanowires with high aspect ratios sets in below a certain minimum diameter when the force due to surface tension exceeds the limit that can lead to plastic flow as determined by the yield stress of the material of the wire. The critical diameter and temperature at which this instability starts and causes the formation of droplets is severely modified by electronic and surface effects. The importance of the surface and electronic structure effects is evidenced by the observation that unbroken Ge nanowires could be encapsulated inside a carbon coating by pyrolysis of organic molecules.[25] To the best of our knowledge, such a postsynthetic encapsulation has not been reported on anisotropic magnetic metallic nano-objects so far.

Here we report an extensive study of the synthesis and thermal stability of the cobalt nanowires, the formation of which was mentioned only briefly in a previous communication.[12] Comparisons to results obtained on cobalt nanorods are also reported.

(14) Lu, A.-H.; Salabas, E. L.; Schüth, F. *Angew. Chem., Int. Ed.* **2007**, *46*(8), 1222.
(15) Zhang, J.; Post, M.; Veres, T.; Jakubek, Z. J.; Guan, J.; Wang, D.; Normandin, F.; Deslandes, Y.; Simard, B. *J. Phys. Chem. B* **2006**, *110*(14), 7122.
(16) Lu, A.-H.; Li, W.-C.; Matoussevitch, N.; Spliethoff, B.; Bonnemann, H.; Schuth, F. *Chem. Commun.* **2005**, 98.
(17) Zalich, M. A.; Baranauskas, V. V.; Riffle, J. S.; Saunders, M.; St. Pierre, T. G. *Chem. Mater.* **2006**, *18*, 2648.
(18) Flahaut, E.; Agnoli, F.; Sloan, J.; O'Connor, C.; Green, M. L. H. *Chem. Mater.* **2002**, *14*, 2553.
(19) Sun, S.; Murray, C. B.; Weller, D.; Folks, L.; Moser, A. *Science* **2000**, *287*, 1989.
(20) Li, Q.; Li, H.; Pol, V. G.; Bruckental, I.; Koltypin, Y.; Calderon-Moreno, J.; Nowike, I.; Gedanken, A. *New J. Chem.* **2003**, *27*, 1194.
(21) Desvaux, C.; Amiens, C.; Fejes, P.; Renaud, P.; Respaud, M.; Lecante, P.; Snoeck, E.; Chaudret, B. *Nat. Mater.* **2005**, *4*, 750.
(22) Toimil-Molares, M. E.; Balogh, A. G.; Cornelius, T. W.; Neumann, R.; Trautmann, C. *Appl. Phys. Lett.* **2004**, *85*, 5337.
(23) Karim, S.; Toimil-Molares, M. E.; Ensinger, W.; Balogh, A. G.; Cornelius, T. W.; Khan, E. U.; Neumann, R. *J. Phys. D* **2007**, *40*, 3767.
(24) Brechignac, C.; Cahuzac, P.; Carlier, F.; Colliex, C.; Leroux, J.; Masson, A.; Yoon, B.; Landman, U. *Phys. Rev. Lett.* **2002**, *88*, 196103.
(25) Wu, Y.; Yang, P. *Appl. Phys. Lett.* **2000**, *77*, 43.

2. Experimental Methods

2.1. Synthesis of Co Nanorods and Nanowires. All synthetic processes have been carried out under an inert Argon atmosphere using classical Schlenk and Fischer−Porter tubes techniques, and argon/vacuum lines. The solvent, anisole (99.7%, Aldrich), was dried over sodium, filtrated, and degassed by a freeze−thaw process prior use. All reactants (oleylamine, 80% −99% primary amines, Aldrich; oleic acid, 99%, Aldrich; lauric acid, 99.5%, Acros-Organics; hexadecylamine, 99%, Aldrich; $Co(\eta^3\text{-}C_8H_{13})(\eta^4\text{-}C_8H_{12})$, Nanomeps; $Co(stearate)_2$, Alfa-Aesar) have been introduced inside a glovebox (O_2 < 1 ppm, H_2O < 1 ppm) as received, to be weighted while avoiding any oxygen or water contamination. Dihydrogen, Air Liquide, contained less than 5 ppm O_2 and 5 ppm H_2O.

Cobalt nanorods have been obtained according to ref 12.

Co nanowires from $Co(\eta^3\text{-}C_8H_{13})(\eta^4\text{-}C_8H_{12})$: 564 mg (2 mmol.) of oleic acid and 0.33 mL (1 mmol.) of oleylamine were dissolved in 20 mL of anisole. After 10 min stirring, this solution was transferred via a canula into a Fischer−Porter bottle containing 276 mg (1 mmol.) of $Co(\eta^3\text{-}C_8H_{13})(\eta^4\text{-}C_8H_{12})$. This mixture was stirred for 20 min to afford a violet solution. It was then pressurized under 3 bar H_2, placed into a heating bath at 150 °C and stirred vigorously for 48hours. At the end of the reaction, excess H_2 was evacuated and the solution cooled down to room temperature. 100 mg of a black precipitate were recovered after filtration, and drying under vacuum. wt %Co: 6.2%.

This reaction was also carried out without stirring during the hydrogenation step.

Co nanowires from $Co(stearate)_2$: 625 mg (1 mmol) of finely powdered Co precursor was dissolved in a solution of 482 mg (2 mmol.) hexadecylamine in 20 mL of anisole. The mixture was stirred for 20 min to afford a violet solution. It was then pressurized under 3 bar H_2, placed into a heating bath at 150 °C, and stirred vigorously for 48hours. At the end of the reaction, excess H_2 was evacuated and the solution cooled to room temperature; 400 mg of a black precipitate were recovered after filtration and drying under a vacuum. The solid was used as such or after dissolution in degassed toluene for further characterizations wt % Co: 8.1%.

2.2. Thermal Annealing. The powder was placed in a ceramic container inside a quartz tube under argon atmosphere. The tube was then closed and placed in an oven. The heating rate was set to either 5 °C/min or 10 °C/min. A plateau was set for 30 min to complete the annealing process. Two temperatures were tested for the plateau: 350 and 500 °C. After annealing, once the tube had spontaneously cooled to room temperature, the powder was recovered in the glovebox.

2.3. Instrumentation. Chemical microanalyses were performed at the CNRS center at Vernaison by ICP-MS (Inductively Coupled Plasma-Mass Spectrometer) after digestion of the samples in concentrated HNO_3, to determine the cobalt content in the materials.

2.4. Transmission Electron Microscopy. The nano-objects were usually deposited on carbon-coated copper grids by casting a drop of a toluene solution of their crude powders. Alternatively, for nonsoluble samples such as annealed materials, a thin slice (70 nm) of the material embedded in a resin was prepared by use of a microtome and directly deposited on a copper grid. Lacey carbon grids were used for HREM investigation. Nickel grids were used for in situ monitoring of the annealing of the nanowires and rods at high temperatures. SEM images were recorded on a JEOL JSM 6700F equipped with a field emission

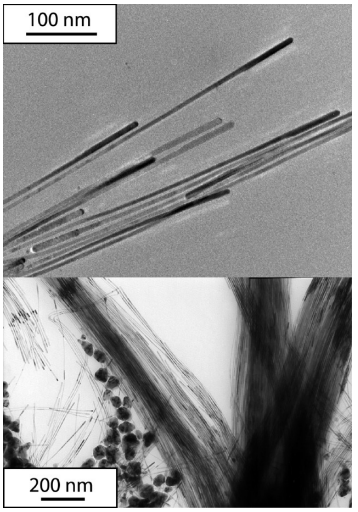

Figure 1. TEM images of cobalt nanowires produced from Co(η^3-C_8H_{13})(η^4-C_8H_{12}).

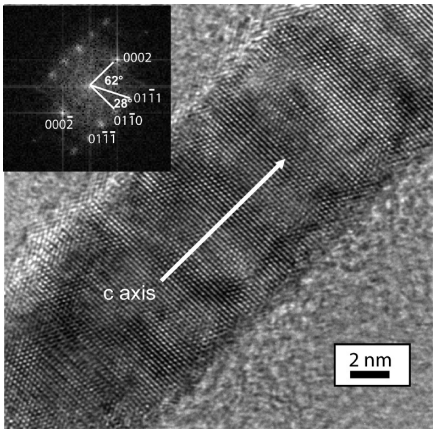

Figure 2. HREM image of a cobalt nanowire produced from Co(η^3-C_8H_{13})(η^4-C_8H_{12}). Inset: Fourier transform of the image.

gun, and TEM images on a JEOL JEM 1011 (100 kV) at the TEMSCAN facility, Université Paul-Sabatier, Toulouse. HREM studies were carried out on a Philips FEI/Tecnai F20ST microscope (field emission gun, Super-Twin lens) with an operating voltage of 200 kV and a point resolution 0.24 nm, in Duisburg. In situ annealing experiments were carried out using CM12/Philips transmission electron microscope with an operating voltage of 120 kV, in Duisburg. A standard Philips single-tilt heating sample holder (PW 6592/00) was applied. The holder permits controlled heating of the sample in the range 20−1000 °C. Specimens are mounted in an annual oven using a conduction Pt rings to ensure good thermal contact. The oven is made of a platinum−rhodium alloy and incorporates a tungsten heating element protected by a cover. Thermal isolation from the rest of the holder is provided by three spherical ceramic mountings. A thermocouple [Pt-PtRh(10%)] measures the oven temperature with an accuracy of ±1 °C. Temperature control and measuring facilities are supplied by the temperature control and measuring unit PW 6313/00.

2.5. Magnetic Measurements. The samples were prepared in the glovebox. The powder was sealed in a gelatin capsule to prevent any oxidation during the transfer of the sample into the magnetometer. Hysteresis loops were recorded on a MPMS Quantum Design SQUID magnetometer at −271 °C (2K), between ±5 T.

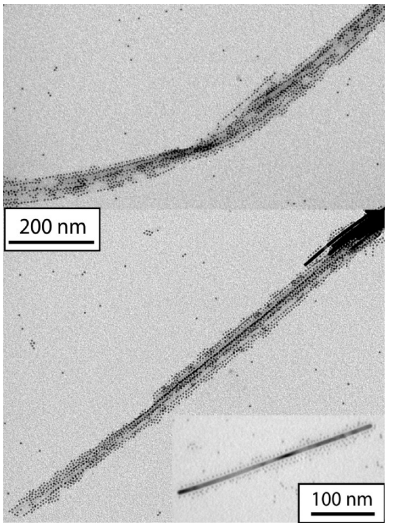

Figure 3. TEM images of the nanowires reacting medium after deposition on a carbon-coated copper grid at an intermediate reaction stage.

Thermogravimetric analyses were carried out on a SETARAM92−16.18 thermobalance in alumina crucibles, operated under a He flow.

Raman spectra were recorded on an Abram HR800 spectrophotometer equipped with a He/Ne laser (7mW on the sample).

UV−vis spectra were recorded on a Shimadzu UV 3100 spectrophotometer. The solutions were prepared in the glovebox in concentration conditions identical to the synthesis ones. The measurement cell was airtight. Co(stearate)$_2$ is poorly soluble in anisole, which accounts for the poor quality of its UV−vis spectrum. The solubility of this complex increases with addition of amine, as does the absorption of the solution. The epsilon values were calculated assuming that all the Co was in solution, they are thus underestimated.

3. Results

Hydrogenation of the organometallic Co(I) complex Co(η^3-C_8H_{13})(η^4-C_8H_{12}), at 150 °C in the presence of 2 equiv. of oleic acid and 1 equiv. of oleylamine, in anisole, under vigorous stirring afforded a black powder stuck to the stirring bar. Figure 1 shows a typical transmission electron microscopy (TEM) image of the material which consists of nanowires with a diameter varying from 7 nm at the center to 9 nm at their ends and lengths of about 1 μm. As already reported, high-resolution TEM (HREM) investigation (Figure 2) evidence lattice planes which are continuous over the whole wire and indicate that it consists of a single crystal, even in the very rare regions where it appears kinked.[26] The Fourier Transform of the HREM image shows a diffraction diagram characteristic of a hcp cobalt structure observed along the [200] direction. This indicates that the nanowires grow along the *c* axis. The measured interplanar distance is identical to that of bulk cobalt: 0.21 nm between (10$\bar{1}$0) planes. Some nanowires are interconnected via large cobalt nodes. HREM investigation of the connections

(26) Snoeck, E.; Dunin-Borkowski, R. E.; Dumestre, F.; Renaud, P.; Amiens, C.; Chaudret, B.; Zurcher, P. *Appl. Phys. Lett.* **2003**, *82*, 88.

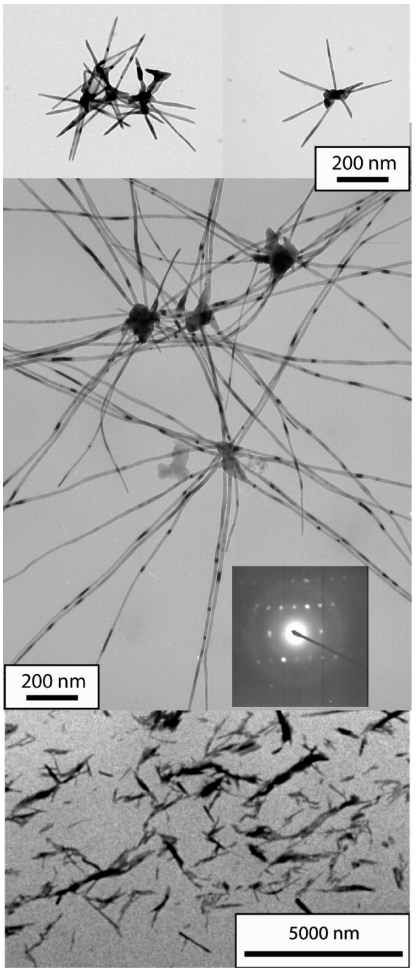

Figure 4. TEM image of cobalt nanowires produced from the Co-(stearate)$_2$ complex. Top, in the presence of 1 equiv. of HDA; middle, in the presence of 2 equiv. of HDA (middle right, SAED on the elongated part showing its hcp structure); bottom, anisotropic supramolecular organization present in reacting medium before hydrogenation (Co(stearate)$_2$ and 2 equiv. of HDA).

evidence their fcc structure. Also some large and isolated fcc nanoparticles could be observed in places.

When the nanowires synthesis was performed without magnetic stirring, we observed an intermediate step in the formation of the nanowires, probably because of a slower kinetics of H_2 transfer into the solution. As Figure 3 shows, cobalt nanoparticles with a diameter of about 3 nm and a very low size distribution self-assemble into 1D superstructures along the long axis of the nanowires suggesting growth via an oriented attachment process.[27]

The main difference in the reaction conditions for the production of long nanowires instead of rods is an increased carboxylic acid content that may promote the formation of intermediate cobalt carboxylate complexes. UV−vis spectra were recorded before submitting the reacting medium to the hydrogen pressure. The spectra (see the Supporting Information, SI1) evidenced the complete conversion of the Co precursor and a large absorption band in the 460−655 nm region with a maximum absorption at 567 nm, and ε value estimated

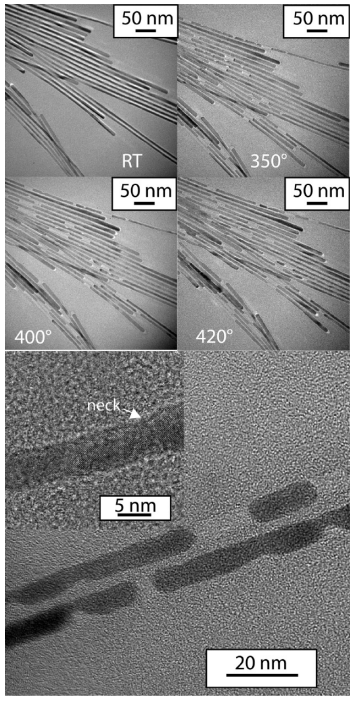

Figure 5. In situ thermal annealing of cobalt nanowires prepared from Co(η^3-C_8H_{13})(η^4-C_8H_{12}) and (bottom) HREM images in the region where they transform.

around 100 cm^{-1} L mol^{-1}. On the sole basis of the spectroscopic study, the nature of the complex could not be established but the cobalt ions are most probably in a mixed carboxylate/amine environment as recently observed for Fe ions in the case of Fe nanoparticles synthesis.[28] Control UV−vis spectra were recorded on mixtures of Co(stearate)$_2$ and respectively 1 or 2 equiv. of amine (see the Supporting Information, SI1). They show very similar patterns, with a maximum absorption at the same wavelength and close ε values of respectively 77 and 92 cm^{-1} L mol^{-1}, confirming the formation of mixed carboxylate/amine complexes in the reacting medium for the synthesis of Co nanowires. Direct decomposition of a carboxylate complex, in the presence of a long chain amine was thus attempted. Hydrogenation of the Co-(stearate)$_2$ complex in the presence of 1 (Figure 4, top) or 2 (Figure 4, middle) equiv. of hexadecylamine, in otherwise identical conditions, afforded also anisotropic growth of Co. The main difference is the characteristic presence of cobalt nodes systematically joining anisotropic branches, which may be the starting point for their growth in this case. HREM investigation reveals again the fcc structure of the nodes, whereas the branches are all of hcp structure. The diameters of the branches is around 8 nm in each case, but their length increases with the amine content in the medium from around 200 nm, when 1equiv. of amine was used, to micrometer long branches in the presence of 2 equiv. of amine. It is noteworthy that in each case, supramolecular assemblies could be evidenced after deposition of the initial reacting medium onto a TEM grid (Figure 4, bottom, and the Supporting

(27) Niederberger, M.; Cölfen, H. *Phys. Chem. Chem. Phys.* **2006**, *8*, 3271.

(28) Lacroix, L.-M.; Lachaize, S.; Falqui, A.; Respaud, M.; Chaudret, B. *J. Am. Chem. Soc.* **2009**, *131*(2), 549.

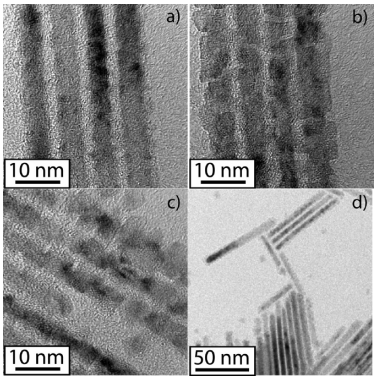

Figure 6. RT behavior of cobalt nanorods in the TEM chamber upon increasing time of observation (a) 5, (b) 10, and (c) 15 min, (d) general view for c.

Information, SI2), whereas no such organization could be observed from a mixture of the ligands, suggesting growth inside a metal-organic supramolecular template.

The thermal behavior of the nanowires was first studied in situ during TEM investigations. The nanowires obtained from $Co(\eta^3\text{-}C_8H_{13})(\eta^4\text{-}C_8H_{12})$ were heated in the microscope. Figure 5 shows localized areas of the nanowires where the metal simply "vanishes", suggesting cobalt evaporation under these high-vacuum conditions.

The inhomogeneity of the evaporation process suggests that the contact between the nanowires and the amorphous carbon layer sustaining them on the TEM grid is not homogeneous itself, providing localized temperature gradients. A closer inspection of this sample by HREM (Figure 5, inset) indicates that the nanowires remain single crystalline throughout the thermal process, even in the region where they start to evaporate. Interestingly, the hcp structure is retained during the whole process, especially no fcc phase could be evidenced, as well as no clear melting step. The thermal behavior is thus closer to sublimation either of cobalt or of a cobalt complex resulting from surface corrosion. Interestingly, the sublimation process occurs at a temperature more than 700 °C lower than in the bulk,[29] evidencing the effect of size reduction on the temperature of change of phase.[30]

Cobalt nanorods (lengths = 60−135 nm, diameter = 4 nm) prepared according to ref 12, i.e., in an analogous chemical environment, were submitted to the same temperature-dependent TEM investigation. A different behavior was expected as it is well-known that the melting and thus evaporation temperatures strongly depend on the size of the nano-objects.[30] Also, these shorter objects would experience a more homogeneous and continuous temperature variation. At time $t = 0$, the rods were single-crystalline with a hcp structure as already published.[12]

After a few minutes, a polycrystalline aspect was observed, then in localized part of the nanorods the evaporation process started. (Figure 6) The evaporation most probably took place where the contact with the carbon support was tighter, similarly to what was observed for the nanowires.

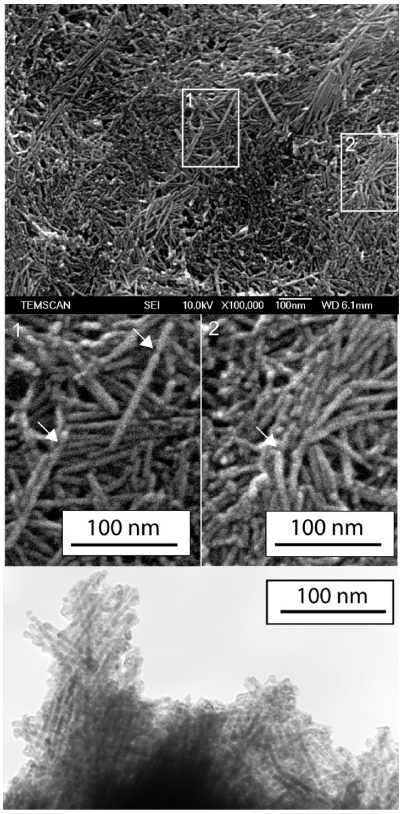

Figure 7. Top, general SEM image of Co nanorods after annealing in the powder from 350 °C; middle, enlargement of regions 1 and 2; bottom, TEM image of the same material.

When the product was annealed in the powder form, under static argon atmosphere, scanning electron microscopy (SEM) investigation showed rodlike objects embedded in an organic matrix, that we assumed to be carbon. (Figure 7) However, a closer inspection by TEM demonstrated that the initial cobalt nanorods were completely fragmented inside a rodlike carbon matrix.

Figure 8(top) shows that bundles of nanowires were still present, as well as the larger initial fcc cobalt nanoparticles, but the facets of the nanowires were rougher. Moreover, many chains of cobalt nanoparticles trapped in a carbon shell could be observed, as a consequence of the fragmentation of the initial nanowires and decomposition of the organic ligands. (middle, Figure 8). HREM was carried out on the annealed samples and showed that the cobalt nanoparticles in the chains retain the hcp structure of the initial nanowires (bottom, Figure 8). When the annealing plateau was set at 500 °C, no nanowires could be evidenced anymore (Figure 9).

Raman spectroscopy was used to study the carbon shell (SI3). After annealing at 350 °C, the two characteristic peaks of a highly amorphous carbon structure were visible at 1330 cm^{-1} (D-band) and at 1697 cm^{-1} (G-band), respectively. Comparison with the Raman spectrum of the nanowires before annealing evidenced that non-decomposed organic ligands remained. This agrees well with the TGA (see the Supporting Information, SI4)

(29) Sales, B. C.; Turner, J. E.; Maple, M. B. *Phys. Rev. Lett.* **1980**, *44* (9), 586.
(30) Moisala, A.; Nasibulin, A. G.; Kauppinen, E. I. *J. Phys.: Condens. Matter* **2003**, *15*, S3011.

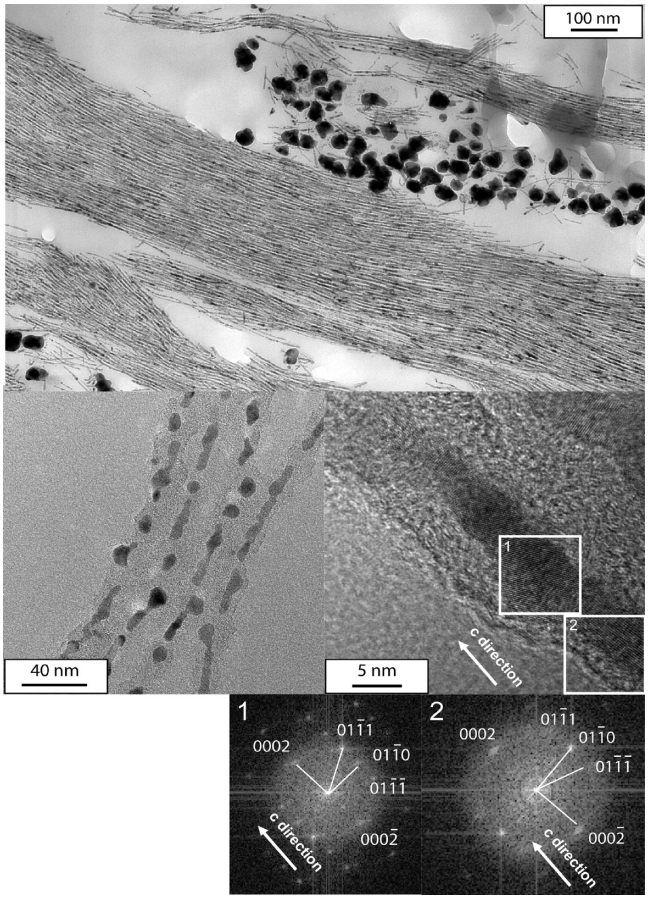

Figure 8. TEM (top) and HREM (middle) images of the material obtained after annealing of Co nanowires under argon at 350 °C (fast temperature ramp); bottom, FT from regions 1 and 2.

experiment, during which full decomposition was observed only at much higher temperature. As the carbon shell was amorphous, we checked if the nano-objects were nevertheless effectively protected against oxidation and retained their magnetic properties upon air exposure. The hysteresis loop for this sample showed a saturation magnetization similar to that of bulk cobalt, indicating that no significant amount of cobalt carbide was formed during the annealing. The coercive field was reduced from 1.7 T (for as prepared nanowires[26]) to 120 mT in agreement with the formation of nano-objects of much lower anisotropy such as nearly spherical nanoparticles. An opening of the loop at 1 T was still visible (arrows on figure 10), demonstrating the presence of some unbroken nanowires. Exposure of the sample to air for 1 month did not lead to any significant decrease of the magnetization demonstrating that the carbon shell effectively protected the nano-objects from oxidation. (Figure 10).

Thermal annealing with a temperature ramp of 5 °C/min and the same plateau at 350 °C resulted in almost no fragmentation of the nanowires. Furthermore a continuous carbon coating was clearly observed by TEM (Figure 11) and HREM (Figure 11 and the Supporting Information, SI5) showed that Co nanowires were not broken; supporting the fact that optimization of the annealing conditions allows the production of air-stable magnetic nanowires.

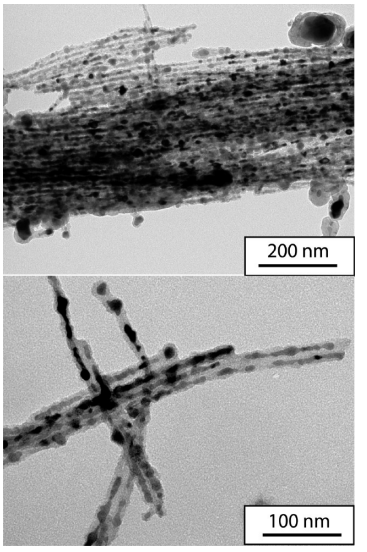

Figure 9. TEM image of the material obtained after annealing of cobalt nanowires at 500 °C under a static Ar atmosphere.

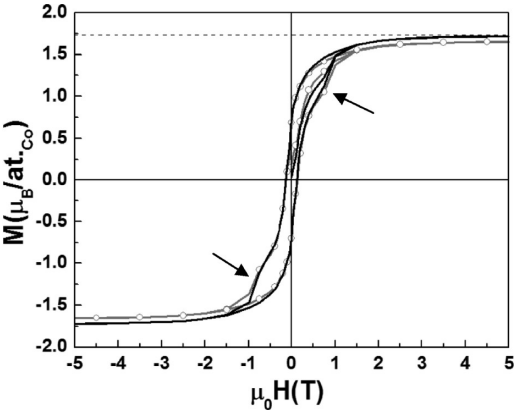

Figure 10. Magnetization loops for cobalt nanowires after annealing at 350 °C (fast temperature ramp): as annealed (black solid line) and after 1 month exposure to air (gray solid line). Horizontal dotted line gives the magnetization for bulk cobalt as a reference.

Discussion

4.1. Formation of Cobalt Nanowires. Generally, the morphogenesis of nanorods or nanowires can result either from the specific coordination of the ligands present in the reacting medium, or from the template effect of anisotropic supramolecular assemblies of ligands or intermediate complexes. These possibilities for the synthesis of the cobalt nano-objects are discussed in the following.

4.1.1. Specific Adsorption of Ligands. In the case of the nanorods, a higher reactivity toward oxygen at their tips was previously observed. Since carboxylate adsorbates act as passivating agents, this suggests that the acid coordinates preferentially along the extended (10$\bar{1}$0) planes of the nanorods.[31] Such a preferential adsorption can be responsible for the anisotropic growth of the nanoparticles into rods or wires either by an atom-by-atom process as discussed by Puntes et al.[11] or following

(31) Rocca, E.; Bertrand, G.; Rapin, C.; Labrune, J. C. *J. Electroanal. Chem.* **2001**, *503*, 133.

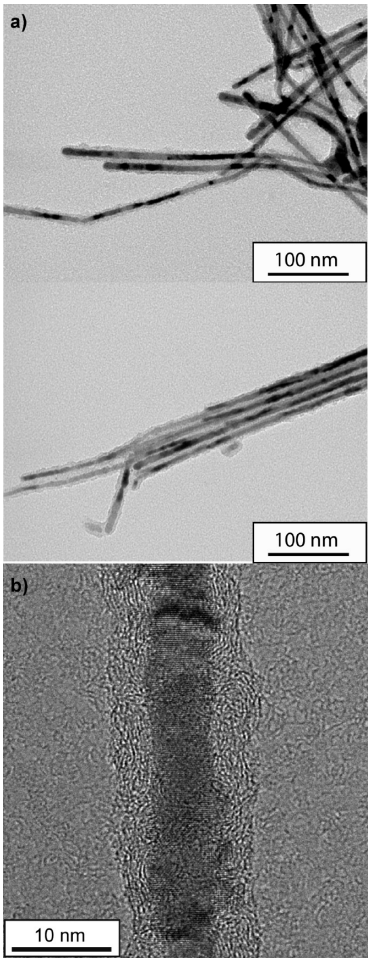

Figure 11. Carbon-coated cobalt nanowires obtained after annealing at 350 °C (slow temperature ramp) under a static Ar atmosphere. (a) TEM and (b) HREM investigations showing the continuity of the structure.

an oriented attachment process of first formed nanoparticles, as described for the formation of CdTe,[32] Pt,[33] TiO_2, ZnO nanowires, and multipodes nanostructures.[27]

4.1.2. Supramolecular Organization of Ligands. Observation of chains of cobalt nanoparticles aligned in the direction of the growth of the nanowires cannot result from an alignment of the nanoparticles along the magnetic stray field. A different figure should be observed in this case as the stray fields form loops from the north to the south pole of the nanowires, or rods.[26] Further, because of the small size of the nanoparticles (< 5 nm), the formation of nanoparticles chains cannot result from magnetic dipolar couplings. As in anisole, a solvent of low dielectric constant and low dipolar moment, the acid and amine ligands form strong acid/base complexes,[34] the formation of chains of cobalt nanoparticles rather suggests two things: first that the ligands can form supramolecular assemblies, the coherence length and robustness of which highly depend on the van der Waals interactions between the parallel chains,[35,36] and second, that the nanorods may grow inside these supramolecular assemblies. Such a process has already been applied for the biotemplated formation of 3 nm large nickel and cobalt nanowires inside the well-known supramolecular assembly of the mosaic virus.[37] However, the formation of rodlike micelles, even from catanionic surfactants, is very unlikely at 150 °C in an organic solvent,[38] ruling out the coalescence of cobalt nanoparticles inside supramolecular assemblies of the ligands as the motor for the anisotropic growth of the nanowires. The critical point at this stage is thus to elucidate the possibility of a *supramolecular assembly of some intermediate metal complex*.

4.1.3. Supramolecular Organization of Intermediate Complexes. Given the reacting medium, the most likely intermediate complex is a mixed amine/alkanoate complex, as suggested by the UV−vis spectroscopy study. Indeed, nanowires, rather than nanorods, form either upon an increase of the acid/amine ratio or directly from the cobalt stearate complex, in the presence of a long chain amine. The critical point is now to elucidate the possibility of a supramolecular assembly of the metal complexes. Homoleptic alkanoate cobalt complexes, often referred to as cobalt soaps, display a high tendency toward self-assembly. For example, they can spread at the water/toluene interface in Langmuir−Blodget cells, with a perpendicular alignment of the alkyl tails with respect to the interface.[39,40] Cobalt alkanoates also present a hexagonal columnar liquid-crystalline mesophase transition above 85−115 °C depending on the length of the alkyl radical,[41] and are further known to polymerize into cylindrical superstructures or form micelles in organic media.[42,43] Still, no study was ever reported on their behavior in the presence of amines. Here, TEM pictures of the reaction medium before hydrogenation evidence anisotropic objects (Figure 4, bottom, and the Supporting Information, SI2), which given their high contrast on the TEM images support the formation of anisotropic supramolecular assemblies of a coordination complex. A similar situation was reported recently for the template synthesis of Fe nanocubes in acid/amine mixtures, and on the basis of Mossbauer spectroscopy, the shape control was attributed to the supramolecular organization of a mixed amine/carboxylate Fe complex.[28] Here, the

(32) Tang, Z.; Kotov, N. A.; Giersig, M. *Science* **2002**, *297*, 237.
(33) Song, Y.; Garcia, R. M.; Dorin, R. M.; Wang, H.; Qiu, Y.; Coker, E. N.; Steen, W. A.; Miller, J. E.; Shelnutt, J. A. *Nano Lett*. **2007**, *7*, 3650.
(34) Klokkenburg, M; Hilhorst, J; Erne, B. H *Vib. Spectrosc*. **2007**, *43*, 243.
(35) Dubois, M.; Demé, B.; Gulik-Krzywicki, T.; Dedieu, J.-C.; Vautrin, C.; Désert, S.; Perez, E.; Zemb, T. *Nature* **2001**, *411*, 672.
(36) McGuiness, C. L.; Blasini, D.; Masejewski, J. P.; Uppili, S.; Cabarcos, O. M.; Smilgies, D.; Allara, D. L. *ACS Nano* **2007**, *1*, 30.
(37) Knez, M.; Bittner, A. M.; Boes, F.; Wege, C.; Jeske, H.; Maib, E.; Kern, K. *Nano Lett*. **2003**, *3*, 1079.
(38) Abecassis, B.; Testard, F.; Arleth, L.; Hansen, S.; Grillo, I.; Zemb, T. *Langmuir* **2006**, *22*, 8017.
(39) Lojewska, J.; Dynarowicz-Latka, P.; Kolodziej, A. *Thin Solid Films* **2006**, *495*, 299.
(40) Hatta, E.; Maekawa, T.; Mukasa, K.; Shimoyama, Y. *Phys. Rev. B* **1999**, *60*, 14561.
(41) Grosshans-Vièlesa, S.; Tihay-Schweyer, F.; Rabub, P.; Paillauda, J.-L.; Braunstein, P.; Lebeau, B.; Estournès, C.; Guille, J.-L.; Rueff, J.-M. *Microporous Mesoporous Mater*. **2007**, *106*, 17.
(42) Zhou, Z.; Georgalis, Y.; Liang, W.; Li, J.; Xu, R.; Chu, B. *J. Colloid Interface Sci*. **1987**, *116*, 473.
(43) Malik, W. U.; Jain, A. K.; Siddiqui, M. J. *Indian J. Chem*. **1976**, *14A*, 906.

supramolecular organization of the mixed amine/carboxylate cobalt complex suggested by the UV−vis spectroscopy and TEM studies could afford a supramolecular reservoir of Co ions, which could act as a template[44] or mediator[45] for the formation of the nanowires.

4.1.4. Role of Dihydrogen. First of all, dihydrogen is mandatory for the production of cobalt atoms by direct reduction of both the initial or intermediate cobalt complexes. Furthermore, the presence of dihydrogen ensures that equilibrium exists between coordinated and noncoordinated acid at the surface of the first formed nanoparticles, i.e., the presence of dihydrogen can favor the coalescence of the first formed nanoparticles. It can also ensure equilibrium between coordinated and noncoordinated acid at the surface of the nanowires formed through the coalescence process and their reconstruction into single-crystalline, well-faceted nanowires. In any case, the presence of dihydrogen is mandatory to ensure completion of the nucleation and anisotropic growth processes.

4.1.5. Co(stearate)$_2$ versus Co(η^3-C_8H_{13})(η^4-C_8H_{12}). The systematic presence of *fcc* nodes for nanowires produced from the cobalt stearate complex, evidence a nucleation process different from the one observed starting from Co(η^3-C_8H_{13})(η^4-C_8H_{12}). When using Co(η^3-C_8H_{13})(η^4-C_8H_{12}) as a precursor, its hydrogenation or, because this complex is thermally unstable, its spontaneous and fast thermal decomposition, can occur in parallel with the formation of the carboxylate complex in the very first stage of the reaction. This would afford cobalt seeds, as already observed in the case of the Co rods synthesis.[12] Reduction of the cobalt carboxylate complex on these seeds (or their coalescence) would then be responsible for the growth of the nanowires. The reduction of the cobalt alkanoate complex can also be responsible for a second nucleation step and generate the larger fcc nanoparticles from which branches and then nanowires would grow. Indeed, the fcc phase is not the stable allotropic form of cobalt at room temperature and it is not surprising that conversion into a hcp structure should occur at a certain growth stage, whatever the growth process.

As a consequence, starlike objects are formed when the cobalt stearate is used as a precursor while bundles of cobalt nanowires are observed when using the Co(η^3-C_8H_{13})(η^4-C_8H_{12}) complex. The formation of bundles of nanowires, which is reminiscent of the self-assembly of the cobalt nanorods produced under similar conditions,[46] is most probably due to quadrupolar interactions as described by Loudet et al.[47] and/or to dipolar magnetic interactions. The van der Waals interactions, as well as possible crystallization of the long alkyl chains of the ligands, will then hold the rods parallel to each others.

4.1.6. Summary. All these observations are in agreement with the following scheme for the morphogenesis of the nanowires. In a first step, a mixed cobalt alkanoate/amine complex is formed which organizes into anisotropic supramolecular assemblies. Upon hydrogenation, the cobalt atoms are produced and form nuclei inside this anisotropic matrix. During this step, carboxylic acid also forms that can adsorb at the surface of the nanoparticles. The preferential coordination of the acid onto the $(10\bar{1}0)$ planes of cobalt (see above) leaves certain facets of the initial nanoparticles available. This can be responsible for a preferential orientation of the first formed nanoparticles inside the supramolecular cobalt soap assemblies. Oriented attachment of the metal nanoparticles would thus lead to the formation of the nanowires.

Finally, it is probable that the morphogenesis of the nanowires involves a complex cooperative process promoted by the preferential coordination of the carboxylic acid onto cobalt surfaces and possibly supramolecular organization of the cobalt intermediate complexes into chains that would act as a reservoir of cobalt atoms.

The arrangement of the nanowires depends mostly on the nucleation step.

4.2. Thermal Behavior of the Nanowires. The thermal behavior of the nanowires prepared from Co(η^3-C_8H_{13})(η^4-C_8H_{12}) was studied as they organize spontaneously into bundles and are thus particularly promising for the formation of permanent magnets.[48] TGA data demonstrate that the nanowires are stable up to 300 °C, which is the limit of thermal stability of most organic polymers, and would thus be suitable for the application envisaged. If the nanowires are heated too fast, or at too elevated temperatures, TEM observations of the annealed powder show that these nanowires fragment into cobalt hcp droplets during the formation of the carbon shell. This suggests that the carbon nanowires undergo Plateau-Rayleigh instability. (Figure 8 and 9) Air stable cobalt nanoparticles, embedded in 1D carbon structures, are obtained at the end of the annealing process.

For comparison, copper nanowires with diameters between 30 and 50 nm start to fragment when the annealing is carried out at 400 °C.[22] C. Bréchignac et al.[24] reported instability and fragmentation of the branches of silver fractals at room temperature. Rayleigh instability is also responsible for the fragmentation of Co nanowires with a diameter close to 54 nm into a chain of nanodroplets upon ion beam bombardment.[49]

Taking into account the low dimensions of the Co nanowires studied here as compared to the literature examples, one could expect their fragmentation at a much lower temperature than that observed, even their room temperature instability. We assume that the Co nanowires are stabilized at room temperature by the organic ligands coordinated at the

(44) Huo, Z.; Tsung, C.-K.; Huang, W.; Zhang, X.; Yang, P. *Nano Lett.* **2008**, *8*(7), 2041.
(45) Lu, X.; Yavuz, M. S.; Tuan, H.-Y.; Korgel, B. A.; Xia, Y. *J. Am. Chem. Soc.* **2008**, *130*, 8900.
(46) Dumestre, F.; Chaudret, B.; Amiens, C.; Respaud, M.; Fejes, P.; Renaud, P.; Zurcher, P. *Angew. Chem., Int. Ed.* **2003**, *42*, 5213–5216.
(47) Loudet, J. C.; Yodh, A. G.; Pouligny, B. *Phys. Rev. B* **2005**, *94*, 018304.
(48) Maurer, T.; Ott, F.; Chaboussant, G.; Soumare, Y.; Piquemal, J.-Y.; Viau, G. *Appl. Phys. Lett.* **2007**, *91*, 172501.
(49) Lian, J.; Wang, L.; Sun, X.; Yu, Q.; Ewing, R. C. *Nano Lett.* **2006**, *6*, 1047.

surface of the nanowires, which thus lowered their surface energy. In contrast to the destabilizing role of the electrostatic charges present on the surface of the gold rods synthesized in the presence of ascorbic acid,[50] here the ligands coordinated onto the surface seem to prevent the diffusion of surface atoms, playing the same role as an oxide layer.[51]

On the other hand, no such fragmentation could be observed in the absence of the ligands, during in situ TEM investigation of the thermal behavior of the nanowires. This suggests that the fragmentation of the nanowires may be linked to the decomposition of the ligands at their surface. Indeed, the presence of adsorbed surface species has been reported in some cases to increase the surface diffusion of the atoms.[52] Here, a carbon shell could be observed on the TEM images of the nanowires annealed under static argon atmosphere (Figures 8, 9, and 11). We propose that, as cobalt is a very efficient catalyst for the formation of carbon nanostructures such as carbon nanotubes, its involvement in the formation of the carbon shell observed here contributes to an increase of the surface diffusion of the atoms. As a comparison, carbon coating of Ge nanowires, which do not display such catalytic properties, could be easily achieved via thermolysis of organic vapors without fragmentation of the nanowires.[25]

In the case of the cobalt nanowires, we could, however, optimize the annealing conditions to favor the formation of the carbon shell over the fragmentation of the nanowires. We based our reasoning on three considerations. First, the melting process of a wire happens in two steps; especially for single-crystalline nanowires, the melting temperature of the surface atoms is lower than that of the bulk.[53,54] Second, the fragmentation of the nanowires implies the mobility of the core atoms. Third, from TGA measurements, the decomposition of the ligands starts at 300 °C. There could then be a temperature window where the ligands would decompose, inducing eventually an increase in the surface diffusion of the surface atoms, but where the core atoms of the nanowires would not have enough mobility for the wire to fragment. The idea was then to give time to a thin carbon shell to form before fragmentation of the nanowires. For this purpose the temperature ramp was set to 5 °C/min instead of 10 °C/min. The annealing plateau was maintained at 350 °C as previously describe, to ensure the formation of a thick enough carbon layer for air protection. Indeed, carbon-coated cobalt nanowires were obtained. (Figure 11) Their surface is irregular indicative of its melting during the annealing process, but only very limited fragmentation was observed in this case. Despite the roughness of the coated nanowires, this is a very promising result, as the carbon coating will preserve their magnetic properties against air oxidation.

The case of the hcp cobalt nanorods is different. From HREM experiments, it is obvious that even a low gain in energy promotes their transformation. This may be related to a lower melting temperature. In agreement with the lower thermal stability of the rods, we could not find annealing conditions affording their carbon coating without inducing the breaking of the rods.

Conclusions

Both Co(η^3-C_8H_{13})(η^4-C_8H_{12}) and Co stearate complexes lead to the formation of cobalt nanowires when reduced under dihydrogen pressure in the presence of long chain acid/amine ligands, demonstrating the crucial role played by the formation of intermediate mixed amine/alkanoate complexes in the first case. However, the nanowires are organized into bundles when prepared from the organometallic complex while they grow from large fcc cobalt particles when prepared from the stearate complex, demonstrating that different nucleation processes are at play. These nanowires are single-crystalline hcp cobalt nanowires of 7−8 nm in diameter and a few μm in length. The coordination of the carboxylate ligands at their surface promotes their stability up to 350 °C, which is compatible with most organic matrices used for the formation of flexible permanent magnets. The nanowires prepared from Co(η^3-C_8H_{13})(η^4-C_8H_{12}) are particularly promising as they organize spontaneously into bundles, enhancing the anisotropy of the material. Careful annealing of these nanowires lead to the formation of a carbon coating without loss of magnetization, protecting the nanowires against air oxidation. From 350 °C, chains of Co nanoparticles embedded in a wirelike carbon matrix are obtained. This fragmentation is the mark of the reconstruction of the nanowires induced by the diffusion of the surface atoms. It may be a consequence of the catalytic role played by cobalt atoms in the formation of the carbon shell during the decomposition of the ligands. These results emphasize the role played by the ligands for the stabilization of nanostructures against Rayleigh instability and/or for the activation of surface diffusion processes.

Acknowledgment. The authors thank C. Routaboul for Raman spectra recording, A. Mari for SQUID Measurements, J. Bonvoisin for access to UV−vis−NIR measurements, V. Colliere for HREM pictures, and R. Backov and P. Rabu for useful discussions. We acknowledge support from the EC via MRTN-CT-2004-005567 "Syntorbmag", http://www.uni-due.de/syntorbmag/ and MEST-CT-2005-020195 "Nanotool", http://www.lcc-toulouse.fr/nanotool/ programs.

Supporting Information Available: UV−vis spectra of the reacting media and reference spectra for the precursors, prior to hydrogenation; TEM images of the anisotropic nano-objects present in the reacting media before hydrogenation; Raman spectra of Co nanowires before and after annealing; TGA of cobalt nanowires; HREM images of carbon coated Co nanowires obtained after annealing at 350 °C (slow temperature ramp) under static Ar atmosphere (PDF). This material is available free of charge via the Internet at http://pubs.acs.org.

(50) Novo, C.; Mulvaney, A. P. *Nano Lett*. **2007**, *7*(2), 520.
(51) Toimil-Molares, M. E.; Karim, S.; Balogh, A. G.; Cornelius, T. W.; Neumann, R.; Sigle, W. In *Trends in Nanotechnology 2005*, Oviedo, Spain, Aug 29−Sept 2, 2005; Phantoms Foundation: Madrid, 2005.
(52) Brechignac, C.; Cahuzac, P.; Carlier, F.; Kebaili, N.; Roux, L.; Masson, A. *Surf. Sci*. **2002**, *518*, 192.
(53) Wen, Y.-H.; Zhu, Z.-Z.; Zhu, R.; Shao, G.-F. *Phys. E* **2004**, *25*, 47.
(54) Miao, L.; Bhethanabotla, V. R.; Joseph, B. *Phys. Rev. B* **2005**, *72*, 134109.